Probing Intradomain and Interdomain Conformational Changes during Equilibrium Unfolding of Phosphoglycerate Kinase: Fluorescence and Circular Dichroism Study of Tryptophan Mutants†

Mark A. Sherman,‡ Joseph M. Beechem,§ and Maria T. Mas*,‡

Division of Biology, Physical Biochemistry Section, Beckman Research Institute of the City of Hope, Duarte, California 91010, and Department of Molecular Physiology and Biophysics, Vanderbilt University, Nashville, Tennessee 37232

Received April 14, 1995; Revised Manuscript Received August 29, 1995⊗

ABSTRACT: Phosphoglycerate kinase is a monomeric protein composed of two globular domains of the α/β type. Extensive domain−domain interactions involve three segments of the polypeptide chain that are distant from one another in the primary sequence: the N-terminus, the C-terminus, and a centrally located α-helix. In order to monitor spectroscopically the conformational changes that occur in the individual domains and at the interdomain interface during the unfolding process, we have constructed a series of single-tryptophan mutants. In addition to two previously described mutants, each with single tryptophans in the C-terminal domain (W308 and W333) [Szpikowska, B. K., Beechem, J. M., Sherman, M. A., & Mas, M. T. (1994) *Biochemistry 33*, 2217−2225], four new single-tryptophan mutants have been constructed: two with tryptophans located in the interdomain region (W194 and W399) and two with tryptophans in the N-terminal domain (W48 and W122). The equilibrium unfolding transitions induced by guanidine hydrochloride were monitored using far-UV CD, near-UV CD, steady-state, and time-resolved fluorescence. These studies reveal two unfolding transitions and suggest a sequential unfolding process for the mutants described in this paper. During the first transition ($C_m \sim 0.5$ M) the interdomain region and C-terminal domain unfold; the N-terminal domain remains relatively compact but lacks much of the tertiary structure that characterizes the native state. A hyperfluorescent intermediate is detected during this transition by tryptophan probes placed within the N-terminal domain. Complete unfolding of the N-terminal domain occurs during the second transition ($C_m \sim 0.9$ M).

Phosphoglycerate kinase, a well-characterized, two-domain enzyme, is an attractive system for studying the role of individual domains and their interactions during the folding process. Both circular dichroism and fluorescence spectroscopy have been used previously to monitor the guanidine-induced unfolding and refolding transitions of wild-type yeast and horse muscle PGK.[1] Although both enzymes have very similar three-dimensional structures (Banks et al., 1979; Watson et al., 1982), their mechanisms of unfolding appear to differ. The unfolding transition of yeast PGK induced by guanidine hydrochloride (Nojima et al., 1976) is highly cooperative. In contrast, two nonoverlapping transitions are observed using far-UV CD and tryptophan fluorescence for horse muscle PGK (Betton et al., 1984), apparently due to a greater stability of the C-terminal domain.

Mutants of yeast PGK with genetically engineered cysteine residues have also been used to probe the equilibrium unfolding/refolding transitions of this protein. After comparing the chemical reactivity of introduced cysteines with ellipticity changes at 218 nm, Yon and co-workers concluded that the hinge region is more sensitive to denaturation by guanidine hydrochloride than either of the two domains (Ballery et al., 1990). Subsequent studies of the refolding kinetics suggested that domain pairing and formation of native tertiary structure occur simultaneously in the slow phase of refolding (Ballery et al., 1993). The existence of a folding intermediate, characterized as having high secondary structure content but lacking a well-defined tertiary structure, has been postulated by these authors (Ballery et al., 1993).

It has been demonstrated that individual yeast PGK domains produced by recombinant DNA methods can fold independently into quasinative structures but fail to reassociate (Missiakas et al., 1990). The C_m value for the guanidine-induced unfolding of the isolated C-terminal domain was found to be lower than for the N-terminal domain, although the structure of the latter appeared to be less compact (Missiakas et al., 1990). The refolding of isolated domains was more rapid than that of the same domains when present in the complete enzyme (Missiakas et al., 1992).

The equilibrium unfolding of yeast PGK and three of its mutants, each lacking one or both native tryptophans (W308 and W333), was studied previously in this laboratory by utilizing circular dichroism (CD), steady-state, and time-resolved fluorescence techniques to examine global and local structural changes induced by guanidine hydrochloride. For each mutant, unfolding transitions monitored by changes in ellipticity at 220 nm were coincident with transitions

†This research was supported in part by the NIH Grants R01 GM41360 and R01 GM37715 (M.T.M.) and R01 GM45990 (J.M.B.). M.T.M. acknowledges partial support by the Cancer Support Grant P01 CA33572 for the Computer Graphics Facility. J.M.B. gratefully acknowledges support from the Lucille P. Markey Foundation.

* Author to whom correspondence should be addressed. Telephone: (818) 301-8347. Fax: (818) 301-8891. E-mail: mmas@coh.org.

‡ Beckman Research Institute of the City of Hope.

§ Vanderbilt University.

⊗ Abstract published in *Advance ACS Abstracts,* October 1, 1995.

[1] Abbreviations: PGK, 3-phosphoglycerate kinase; CD, circular dichroism; Gdn-HCl, guanidine hydrochloride, WT, wild-type.

0006-2960/95/0434-13934$09.00/0

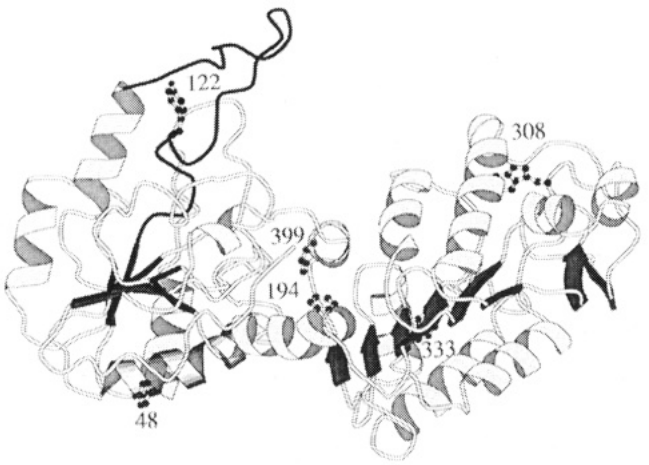

FIGURE 1: Ribbon diagram of yeast phosphoglycerate kinase showing the positions of the two native tryptophans (W308, W333; C-domain) and the residues mutated to tryptophan for this study [F194, interdomain helix; L399, hinge-spanning C-terminus; Y48, N-domain, helix I (shaded); and Y122, N-domain, extended loop (black)]. The figure was drawn with the program MOLSCRIPT (Kraulis, 1991) using coordinates from Brookhaven file 3PGK (Watson et al., 1982).

monitored by changes in tryptophan fluorescence emission intensity. A two-state unfolding model was most consistent with the data from this study. Time-resolved fluorescence measurements yielded transition midpoint (C_m) values that were virtually identical to values obtained from steady-state measurements. However, these studies did not confirm the presence of a hyperfluorescent intermediate in wild-type PGK reported in an earlier study (Missiakas et al., 1990).

Genetic engineering techniques have been used in the present study to introduce single tryptophan residues at new locations in the PGK structure as probes of local conformational changes. In addition to the two previously described mutants containing single tryptophans in the C-terminal domain (W308 and W333) and a no-tryptophan mutant (W−) (Szpikowska et al., 1994), four new single-tryptophan mutants have been constructed, two with a tryptophan located in the N-terminal domain (W48 and W122) and two in the interdomain region (W194 and W399) (Figure 1). Two double-tryptophan mutants (W48/W308 and W48/W333), containing one tryptophan in each domain, have also been constructed and included in this study. The equilibrium unfolding transitions of these mutants have been investigated using far-UV CD, near-UV CD, and steady-state, and time-resolved fluorescence in an effort to further characterize the conformational changes that occur under equilibrium conditions during guanidine hydrochloride induced unfolding. Stopped-flow kinetic studies of these mutants are described in the accompanying paper (Beechem et al., 1995).

EXPERIMENTAL PROCEDURES

Reagents. Guanidine hydrochloride (sequanal grade) was purchased from Pierce. L-Tryptophan was from Aldrich Chemical Co. Sodium phosphate (monobasic and dibasic) was from J. T. Baker. The source of reagents used in the PGK assay was as reported previously (Mas et al., 1987, 1988).

Construction, Expression, and Purification of Single- and Double-Tryptophan Mutants. Site-directed mutagenesis experiments, yeast expression, and purification of mutant proteins were performed using previously described procedures (Mas et al., 1986, 1987, 1988). A PGK gene in which both native tryptophans have been replaced with phenylalanines (W−; Szpikowska et al., 1994) was used as the template for constructing the mutants described in this paper. Two tyrosines located in the N-terminal domain, Y48 and Y122, were selected for replacement. Both are partially exposed to solvent and surrounded by one or more charged residues, yet each is situated on opposite sides of the domain. Two double-tryptophan mutants, W48/W308 and W48/W333, were also created so that a single probe would be present in each domain of the same protein. Mutants with single tryptophans located in the interdomain hinge region were also constructed. W194 and W399 replace F194 and L399, respectively. Both are buried and pack against each other in the native structure (Figure 1) but belong to different secondary structure elements.

Determination of Specific Activity. Enzyme activity in the direction of formation of 1,3-diphosphoglycerate was measured spectrophotometrically at 25 °C as previously described (Mas et al., 1986), in the absence of sulfate.

Determination of Molar Extinction Coefficients. Molar extinction coefficients at 280 nm were determined with a Uvikon 860 spectrophotometer (Kontron) using the method of Gill and von Hippel (1989).

CD Measurements. Circular dichroism experiments were carried out using a Jasco-600 spectropolarimeter and quartz cuvettes of 1 mm (far UV) or 10 mm (near UV) path length. Protein solutions (0.1 mg/mL, far UV; 1.0 mg/mL, near UV) were prepared in 20 mM sodium phosphate buffer, pH 7.50. Four scans (far UV) or ten scans (near UV) were recorded for each sample at a scan speed of 20 nm/min and a bandwidth of 1 nm. The scans were averaged and corrected for buffer baseline. Molar residue ellipticity values $[\theta]_{MRW}$ (expressed in deg cm^2 dmol^{-1}) were calculated using a molecular weight of 44 700 for PGK ($n = 415$ amino acids) (Hitzeman et al., 1982). Ellipticity (θ, in mdeg), measured in the near-UV CD range, was converted to $\Delta\epsilon$ (M^{-1} cm^{-1}) as described by Schmid (1989).

Fluorescence Measurements. Steady-state fluorescence measurements were performed at 25 °C using a Fluorolog-2 photon counting spectrofluorometer (Spex Industries, Edison, NJ). All measurements were conducted in the ratio mode with 5-nm bandwidths for both the excitation and emission monochromators. Steady-state fluorescence emission spectra were recorded at a scan rate of 1 nm/s. The emission spectra were acquired at an excitation wavelength of 295 nm, in the 300−450 nm range. Background fluorescence from buffer and denaturant was also recorded and subtracted from the protein spectra. Time-resolved fluorescence measurements were performed as described previously (Szpikowska et al., 1994).

Determination of Tryptophan Quantum Yields. Tryptophan quantum yields were determined at 25 °C relative to a value of 0.14 for tryptophan in water (Kirby & Steiner, 1970), as previously described (Szpikowska et al., 1994).

Equilibrium Unfolding Experiments. Unfolding transitions were monitored using circular dichroism (CD), and steady-state, and time-resolved fluorescence techniques. The equilibrium unfolding data were obtained for protein solutions at 0.1 mg/mL in 20 mM sodium phosphate, pH 7.5, by monitoring the ellipticity at 220 nm and total fluorescence emission intensity (area under the emission peak from 305 to 450 nm; excitation at 295 nm). Protein solutions were incubated at least 3 h at room temperature in the presence

Table 1: Specific Activities and Spectral Properties of PGK Mutants[a]

mutant	specific activity (units/mg)	mean residue ellipticity (deg cm^2 dmol^{-1})		extinction coefficients		fluorescence emission maxima (nm)[b] at			tryptophan quantum yield Q[c]
		$[\theta]_{208nm}$	$[\theta]_{220nm}$	ϵ_{280nm} (M^{-1} cm^{-1})	$A_{280}^{0.1\%}$ (mg^{-1} mL cm^{-1})	0 M Gdn-HCl	maximum intensity	4 M Gdn-HCl	
W194	394	−10792	−11191	17433	0.39	328		355	0.393
W399	243	−9834	−9101	16092	0.36	339		355	0.206
W48	381	−8843	−8401	14304	0.32	342	347	357	0.116
W122	562	−9618	−9478	13410	0.30	330	341	355	0.045
W48/W308	703	−10642	−11363	20562	0.46	342	348	356	nd
W48/W333	445	−10965	−10986	20562	0.46	339	349	355	nd
W308[d]	576	−10717	−10750	16986	0.38	339		355	0.038
W333[d]	356	−11525	−11116	16986	0.38	317		356	0.020
W−[d]	448	−9900	−9890	10728	0.24	nd	nd	nd	nd

[a] Spectral measurements were performed in 20 mM sodium phosphate buffer, pH 7.5. Enzymatic activity measurements were carried out as described in the text. [b] λ_{ex} = 295 nm; data represent uncorrected values. [c] Quantum yields relative to tryptophan in water (Q = 0.14). [d] Data from Szpikowska et al. (1994).

of various concentrations of Gdn-HCl (0−4 M) to ensure that equilibrium had been reached. Longer incubation times (up to 24 h) produced no further changes in the fluorescence and CD signals. The spectra of solutions lacking protein were measured in parallel for each sample and subtracted from the spectra of the protein sample. Conditions of the time-resolved fluorescence experiments were as described by Szpikowska et al. (1994). Renaturation experiments were performed to verify the reversibility of the unfolding transitions. Renaturation of proteins unfolded in 6 M Gdn-HCl was performed as described by Missiakas et al. (1990). In these experiments, the unfolded proteins were diluted to a series of final denaturant concentrations (between 0 and 6 M Gdn-HCl) and incubated for 5 h prior to spectral measurements. The final protein concentration of each renatured sample was the same as in the equilibrium unfolding experiments (0.1 mg/mL).

Analysis of the Unfolding Transitions. Guanidine-induced unfolding transitions were analyzed using Marquardt's nonlinear least-squares algorithm (Sigma Plot 5.0; Jandel Sci., San Rafael, CA) to fit the experimental data to a two- or three-state unfolding model as described previously (Mas et al., 1995). The second transition midpoint in the far-UV CD unfolding curves is more difficult to determine due to low amplitude of this minor but undisputable transition and to a decreased signal/noise at high denaturant concentration. It was clear from examination of the data that the second transition was not simply a baseline effect. However, when baseline correction terms were included in the curve fitting equation, the entire second transition was incorporated into the upper baseline term. For this reason, in the analysis of the CD data according to a three-state model, baseline slopes, s_N and s_U, were fixed at zero. This simplification appears justified because the effects of Gdn-HCl on the far-UV signal of the folded and unfolded states are relatively small (less than 10%) for the data gathered between 0 and 4 M.

RESULTS

Enzymatic Activities and Spectral Properties of W48, W122, W194, W399, W48/W308, and W48/W333 PGK Mutants. Specific activities for the W48, W122, W194, W399, W48/W308, and W48/W333 mutants are listed in Table 1. Most are similar to or better than those previously reported for W− and WT PGK. The activity of the W399 mutant is significantly less than that of the W− mutant, despite the fact that the far UV-CD spectra for these two mutants are virtually the same (see below). This might be due to altered packing of the C-terminus against the hinge helix and against the N-terminal domain, previously shown to be important for activity (Mas & Resplandor, 1988).

Molar residue ellipticities at 208 and 220 nm minima of the far-UV CD spectra are also given in Table 1. The far-UV CD spectra are similar for all proteins, suggesting that their secondary structures are similar. The small differences observed in ellipticities at the two minima might be due to differences in their aromatic amino acid content (Woody, 1978; Manning & Woody, 1989; Chakrabartty et al., 1993). Table 1 also lists the extinction coefficients at 280 nm determined according to Gill and von Hippel (1989) and tryptophan quantum yields determined relative to tryptophan in water.

The two single tryptophan mutants with tryptophans situated in the interdomain region (W194 and W399) have the highest quantum yield (0.39 and 0.21, respectively; Table 1) and both exhibit a significant decrease in emission intensity upon unfolding, in addition to a red-shift of the emission maximum. In contrast, the two N-domain tryptophans, W122 and W48, are quenched in the folded state (Q = 0.04 and 0.12, respectively), and their emission intensity increases upon unfolding. In contrast to the W194 and W399 mutants, for which maximum emission is observed in the folded form, the W48, W122, W48/W308, and W48/W333 mutants exhibit maximum emission intensities at intermediate Gdn-HCl concentrations. The wavelength of the emission maximum in the spectrum of this hyperfluorescent intermediate is longer than in the spectrum of the folded protein (at 0 M Gdn-HCl) but shorter than in the spectrum of the completely unfolded protein (at 4 M Gdn-HCl). The emission maximum in the spectra of all unfolded mutants undergoes a red-shift to 355 nm (Table 1).

Guanidine-Induced Equilibrium Unfolding Transitions Monitored by Fluorescence and CD. Figure 2 and Table 2 show the equilibrium unfolding data for all single- and double-tryptophan containing PGK mutants described in this paper. In Figure 2, total fluorescence emission intensity (305−450 nm) and ellipticity changes at 220 nm for each mutant are plotted as a function of Gdn-HCl concentration (0−2 M). Far-UV CD spectra were recorded after incubation of samples under conditions identical to those used for unfolding the samples prior to fluorescence intensity measurements. The plots are superimposed to emphasize the coincident transitions derived from both methods. The fluorescence data have been normalized so that 0 and 1 correspond to the minimum and maximum observed signal,

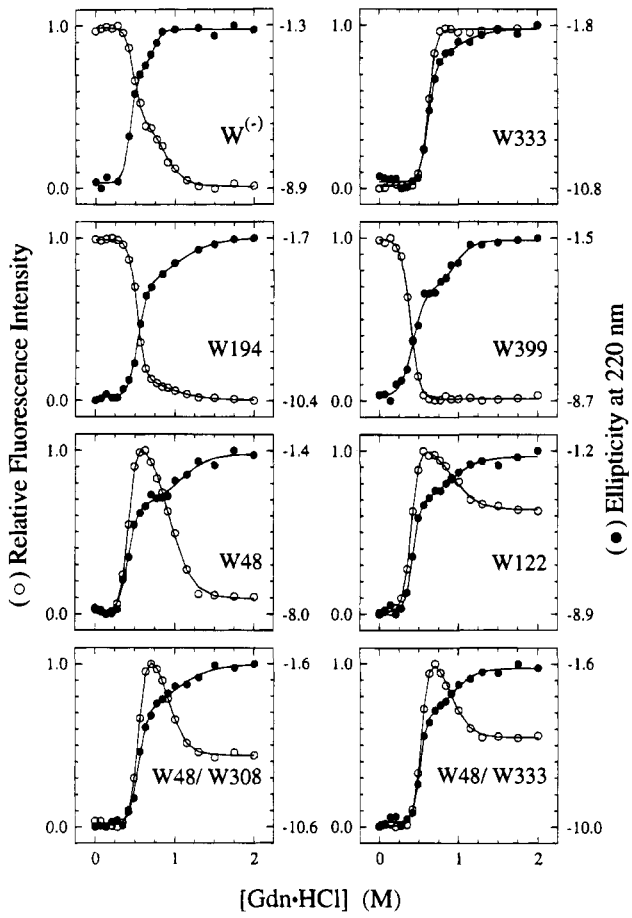

FIGURE 2: Guanidine hydrochloride induced equilibrium unfolding profiles for the no-tryptophan (W−), single-tryptophan (W333, W194, W399, W48, W122), and double-tryptophan (W48/W308, W48/W333) PGK mutants. For each mutant, total fluorescence emission intensities (arbitrary units), measured at 295 nm excitation wavelength (280 nm for the W− mutant), are plotted as a function of denaturant concentration (○). Background fluorescence due to solvent alone (buffer solution containing identical denaturant concentration) was subtracted from each protein spectrum. Ellipticity (in deg cm^2 dmol^{-1}) at 220 nm, obtained from far-UV CD spectra of protein samples after solvent baseline subtraction, is also plotted (●). The relative values of 0 and 1 correspond to the minimum and maximum observed signal, respectively. No correction of the pre- and posttransition baseline slopes was performed. The plots are superimposed to emphasize the fact that the unfolding transitions monitored by both methods coincide. The experimental conditions were the same for each method (protein at 0.1 mg/mL in 20 mM sodium phosphate, pH 7.5, 25 °C). Solid lines represent nonlinear least-squares fits to a three-state (two transition) model for all data except the W333 and W399 fluorescence data, for which a two-state (single transition) model was employed.

respectively. The solid lines represent nonlinear least-squares fits to the data as described under Experimental Procedures. A three state model (N, I, and U) was adopted whenever a two-state model (N and U) failed to adequately describe the data (i.e., transitions were asymmetric or distinctly biphasic).

(1) Unfolding Transitions Monitored by Steady-State Fluorescence. Unlike ellipticity changes, where the signal becomes increasingly less negative upon unfolding, the direction of fluorescence intensity change varies from mutant to mutant. Tryptophan fluorescence emission intensity (or tyrosine fluorescence in the case of W−) decreases upon unfolding for the W194, W399, and W− mutants and increases with increasing denaturant concentration for the other mutants (Figure 2).

The W122 and W48 unfolding curves are clearly biphasic, yielding two distinct C_m values which are identical for both mutants (Table 2). Transition midpoints occur at 0.40 and 0.91 M guanidine concentration for both tryptophans, despite their positions on opposite sides of the N-terminal domain.

Two transitions were also observed in the fluorescence-detected unfolding curves of the W48/W333 and W48/W308 double mutants, and the transitions were virtually identical (0.54 and 0.90 M) for both mutants. Comparing the transition midpoints calculated from the W48 single tryptophan fluorescence data (0.41 and 0.90 M) to those from the double mutants suggests that the addition of tryptophans to the C-terminal domain shifts the first transition to a slightly higher concentration of Gdn-HCl but has no effect on the second transition. A close examination of the data reveals that the unfolding profile of the W194 mutant is also biphasic. However, 86% of the maximum signal change is due to the first unfolding transition.

In contrast, the W399 unfolding profile is clearly monophasic, as were the previously reported W308 and W333 single-mutant curves [Figure 5 in Szpikowska et al. (1994)]. Interestingly, the two hinge tryptophans (W194 and W399) experience changes in environment at distinctly different concentrations of Gdn-HCl (C_m = 0.52 and 0.39), despite their expected similar environment at the interface between two helices in the hinge. However, it should be pointed out that the environment of W399 appears to be less hydrophobic than W194, as indicated by their different emission maxima (339 and 328 nm, respectively). This suggests that the packing of the C-terminal tail may have been perturbed by the L399W mutation, resulting in greater solvent exposure and destabilization of the hinge. Also note that W194 belongs to the helix which begins in the N-domain and ends in the C-domain. W194 is therefore more likely to sense changes in both domains compared to W399, which belongs to the C-terminal tail that spans the hinge region.

(2) Unfolding Transitions Monitored by Far-UV Circular Dichroism. Unlike fluorescence emission measurements at λ_{ex} = 295 nm, which are sensitive to changes in the local environment of tryptophans, changes in the far-UV CD spectrum upon addition of Gdn-HCl are believed to primarily reflect changes in the secondary structure (peptide backbone) of the entire protein although aromatic residues may also contribute in this region (Woody, 1978; Manning & Woody, 1989; Chakrabartty, 1993).

When CD is used to monitor unfolding (Figure 2), two transitions are observed for all single tryptophan mutants with tryptophans located in N-domain and hinge (W48, W122, W194, and W399) as well as the two double tryptophan mutants (W48/W308 and W48/W333). The first transition consistently represents ~65% of the observed signal. With the exception of the W194 mutant, the first phase for all single tryptophan mutants has its midpoint centered around 0.42 M Gdn-HCl, identical to the value obtained for the parent mutant (W−) when analyzed in a similar manner. For the W194 mutant, the first transition occurs at a significantly higher guanidine concentration (C_m value of 0.53 M), perhaps due to tighter packing in the hinge region.

The second transition midpoint for each far-UV CD unfolding curve is more difficult to determine due to signal noise experienced at high concentrations of Gdn-HCl and low amplitude of the second transition but is typically centered around 1.0 ± 0.15 M for all mutants studied, including the double tryptophan mutants. Two transitions

Table 2: Free Energy Changes,[a] Denaturant Concentration Indexes,[a] and Transition Midpoints[b] for Gdn-HCl-Induced Unfolding Transitions in Phosphate Buffer As Monitored by Fluorescence and CD

mutant	$\Delta G^{\circ}_{o,N\rightarrow U}$ (kcal/mol)	$m_{N\rightarrow U}$ (kcal/mol·M)	$\Delta G^{\circ}_{o,N\rightarrow I}$ (kcal/mol)	$m_{N\rightarrow I}$ (kcal/mol·M)	$\Delta G^{\circ}_{o,I\rightarrow U}$ (kcal/mol)	$m_{I\rightarrow U}$ (kcal/mol·M)	C_{m1} (M)	C_{m2} (M)
				Fluorescence				
W194			6.30 ± 0.28	12.1 ± 0.6	2.68 ± 2.14	2.9 ± 1.7	0.52 ± 0.01	0.91 ± 0.2
W399	4.15 ± 0.18	10.7 ± 0.5					0.39 ± 0.01	
W48			5.31 ± 0.37	12.7 ± 0.9	3.80 ± 0.36	4.1 ± 0.3	0.42 ± 0.01	0.92 ± 0.01
W122			4.81 ± 0.24	11.9 ± 0.6	3.45 ± 0.58	3.8 ± 0.5	0.40 ± 0.01	0.91 ± 0.03
W48/W308			6.84 ± 0.35	12.7 ± 0.7	4.94 ± 0.57	5.4 ± 0.5	0.54 ± 0.01	0.92 ± 0.01
W48/W333			6.85 ± 0.30	12.9 ± 0.6	4.45 ± 0.57	5.0 ± 0.5	0.53 ± 0.01	0.90 ± 0.02
W308	9.42 ± 1.39	14.8 ± 2.2					0.64 ± 0.01	
W333	7.66 ± 0.36	12.4 ± 0.6					0.62 ± 0.01	
W−			5.38 ± 0.74	12.1 ± 1.7	4.36 ± 1.16	5.1 ± 1.1	0.48 ± 0.01	0.86 ± 0..04
				Circular Dichroism				
W194			5.44 ± 0.48	10.2 ± 0.9	2.33 ± 1.52	2.4 ± 1.1	0.53 ± 0.01	0.97 ± 0.20
W399			3.40 ± 0.56	8.1 ± 1.5	5.06 ± 2.41	5.3 ± 2.3	0.42 ± 0.02	0.95 ± 0.06
W48			4.31 ± 0.67	10.5 ± 1.7	3.54 ± 1.58	3.3 ± 1.3	0.41 ± 0.01	1.06 ± 0.08
W122[c]			5.79 ± 0.76	13.7 ± 1.8	2.72 ± 1.41	3.2 ± 1.3	0.42 ± 0.01	0.86 ± 0.10
W48/W308[c]			5.93 ± 0.72	10.9 ± 1.3	2.34 ± 2.02	2.4 ± 1.5	0.55 ± 0.01	0.96 ± 0.27
W48/W333[c]			7.89 ± 1.06	15.4 ± 2.1	3.64 ± 1.56	4.0 ± 1.4	0.51 ± 0.01	0.91 ± 0.08
W308[c]			6.85 ± 0.08	10.9 ± 2.2	4.87 ± 0.11	5.8 ± 4.9	0.62 ± 0.03	0.84 ± 0.27
W333[c]			7.48 ± 1.03	11.9 ± 1.7	1.95 ± 4.09	2.4 ± 2.6	0.63 ± 0.05	0.82 ± 0.83
W−			6.08 ± 1.19	14.0 ± 2.9	8.37 ± 3.89	11.5 ± 5.0	0.43 ± 0.01	0.73 ± 0.03

[a] Calculated as described in Experimental Procedures. Values reported are ± one standard deviation. $\Delta G^{\circ}_{o,N\rightarrow I}$ and $\Delta G^{\circ}_{o,I\rightarrow U}$ are the free energy changes for the native to intermediate and intermediate to unfolded transitions, respectively, in the absence of denaturant at the reference temperature (25 °C), and $m_{N\rightarrow I}$ and $m_{I\rightarrow U}$ are the corresponding denaturant index values which describe the dependence of the standard free energy changes on denaturant concentration (Eftink et al., 1994). [b] Calculated using the relationship $C_m = \Delta G^{\circ}_o/m$. [c] Fraction of change at 220 nm attributed to the N → I transition fixed at 0.65 during curve fitting.

(Table 2) are also observed in the CD unfolding curves of the W−, W308, and W333 mutants upon careful re-examination of existing data [see Figure 5 in Szpikowska et al. (1994)]. The second transition, visible as a slight flattening of the curve's upper shoulder, is easily overlooked and is largely eliminated if baseline correction techniques are applied to the data prior to curve fitting. Note, however, that the unfolding curve for wild-type PGK is clearly monophasic, with no indication of asymmetry in the upper shoulder.

(3) Comparison of the Unfolding Transitions Derived from Fluorescence and CD Experiments. Examination of the unfolding transition data (Table 2 and Figure 2) indicates that when steady-state fluorescence intensity is used to monitor unfolding, two phases are seen only when the fluorescent probe is located in, or adjacent to, the N-terminal domain (for the W− mutant, the "probe" is actually seven tyrosine residues, five of which are located in the N-terminal domain). When CD is used to monitor unfolding, two phases are seen for all mutants which lack either one or both of the native tryptophans, regardless of whether unfolding curves derived from fluorescence data are monophasic or biphasic. In cases where two transitions are present both in the fluorescence intensity data and the CD data, both C_m values are coincident. In cases where one transition is apparent in the fluorescence-monitored unfolding curve and two are apparent in the corresponding CD-monitored unfolding curve, the C_m value extracted from the fluorescence data coincides with the first of the two C_m values calculated from the CD data. It therefore appears that fluorescent probes located in the C-domain or C-terminus are able to monitor only one of the unfolding transitions (the first), even though CD data suggest that two transitions are present, whereas fluorescent probes located in the N-domain or trans-domain helix are able to monitor both. Future experiments will determine if a single or double transition is detected by additional single tryptophans, depending on their location in the C-terminal domain.

(4) Unfolding Transitions Monitored by Time-Resolved Fluorescence. Equilibrium time-resolved fluorescence titrations were performed on all tryptophan-containing PGK mutants in order to examine the time-resolved rotational and lifetime properties as a function of Gdn-HCl. A complete analysis of the time-resolved equilibrium titrations of a typical amino-terminal domain tryptophan (W48), hinge domain tryptophan (W399), and carboxy-terminal domain tryptophan (W308) are shown in Figure 3A−C. The rotational markers (β, ϕ in Figure 3A) for W48 reveal how invariant these parameters are from 0 to 0.8 M Gdn-HCl, in the region of the first transition detected by fluorescence intensity and ellipticity changes (Figure 2). It appears, however, that the W48 tryptophan lifetimes (especially the longest lifetime term) sense both transitions (see arrows in Figure 3A). Both the hinge region tryptophan (Figure 3B) and the carboxy-terminal tryptophan (Figure 3C) rotational markers parallel the observed total intensity signal changes. The hinge tryptophan (Figure 3B) requires only two fluorescence lifetime terms, whereas all of the other tryptophan mutants require at least three lifetime terms. The amplitudes for the hinge tryptophan (W399) long lifetime term are dominated by the initial carboxy-terminal domain unfolding but do reveal an additional shift in amplitude consistent with the unfolding of the amino-terminal domain (see Figure 3B). The carboxy-terminal domain tryptophans (Figure 3C) clearly reveal that the total intensity change and anisotropy change occur in the low Gdn-HCl concentration range compared to the amino-terminal domain tryptophans (Figure 3A). For a full discussion of the time-resolved titrations for the carboxy-terminal domain tryptophans [W308, W333, and wild-type; see Szpikowska et al. (1994)].

If one overlaps the titrations from all of the various mutants which have been examined together (both single tryptophan and double-tryptophan mutants), one can observe that they

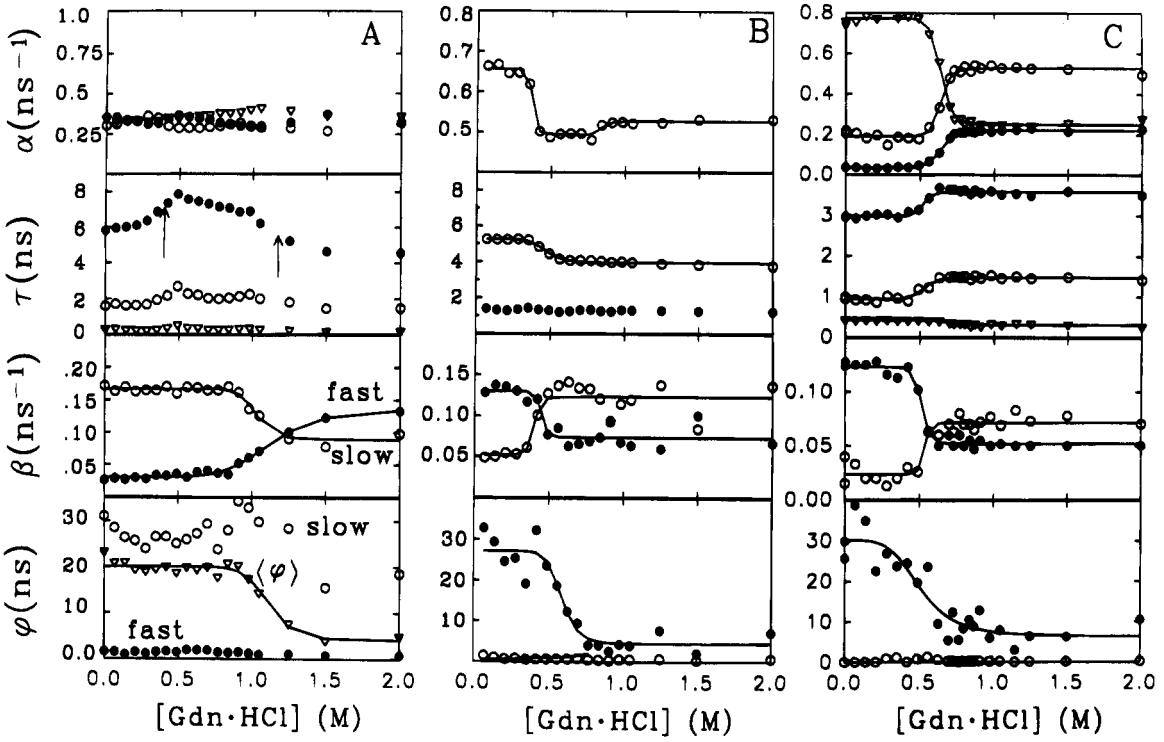

FIGURE 3: Equilibrium unfolding transitions monitored by time-resolved fluorescence total intensity and anisotropy: (A) amino-terminal domain (W48); (B) hinge region (W399); (C) carboxy-terminal domain (W308). Time-resolved fluorescence measurements were performed as previously described (Szpikowska et al., 1994). Population amplitudes (α), lifetimes (τ), rotational amplitudes (β), and rotational correlation times (ϕ) are shown as a function of Gdn-HCl concentration. Population amplitudes and lifetime symbols are grouped together, as are the rotational correlation times and rotational amplitude terms. Multiple lifetimes recovered for individual tryptophans and the corresponding population amplitudes are plotted using different symbols. Arrows in panel A represent the approximate centers of the low and high Gdn-HCl transitions observed from steady-state total intensity fluorescence. All experiments were performed in 20 mM sodium phosphate buffer, pH 7.5, at 25 °C and 1−2 mg/mL protein concentration.

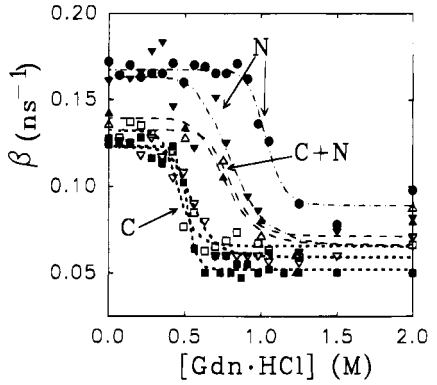

FIGURE 4: Rotational amplitudes (β) associated with the recovered slow rotational correlation time of all of the carboxy-terminal domain mutants [C →; W308 (□), W333 (■), WT (▽)], double-tryptophan mutants [C + N →; W48/W308 (△), W48/W333 (▲)], and the amino-terminal domain mutants [N →; W122 (▼), W48 (●)] as a function of Gdn-HCl concentration.

fall into three distinct classes (see Figure 4). For this figure, the pre-exponential associated with the slowest motion term of the anisotropy is plotted as a function of Gdn-HCl concentration. Rather strikingly, the C-terminal domain markers (W308, W333) cluster around 0.45−0.55 M C_m, the double mutants containing both an amino- and carboxy-domain marker have intermediate 0.7−0.8 M C_m's, and the amino-terminal markers are the most stable with a C_m of W122 = 0.9 M and W48 = 1.03 M. Remarkably, the time-resolved fluorescence anisotropy in the amino-terminal domain is almost invariant as the carboxy-terminal domain unfolds. This is probably due to the relatively short mean lifetime of these tryptophans ($\langle\tau\rangle$), relative to the global motion (ϕ) of the entire protein [$\langle\tau\rangle/\phi$ = (3.1 ns/30 ns)]. It may also be possible that both domains are not hydrodynamically coupled to each other.

(5) Effect of Guanidine Hydrochloride on the Near-UV CD Spectra. Protein absorbance bands in the near-UV range (250−310 nm) can be attributed to aromatic amino acids. Changes in ellipticity associated with these residues upon exposure to denaturant or other perturbations are thought to reflect local changes in tertiary structure. Five of the seven tyrosines in yeast PGK are located in the N-domain, one in the hinge, and one in the C-domain [see Figure 1 in Szpikowska et al. (1994)]. Positions of tryptophans in the proteins examined in this study are indicated in Figure 1.

Near-UV CD spectra for the W− and tryptophan-containing PGK mutants were recorded in the presence of 0, 0.5, 1.0, 1.5, and 2.0 M Gdn-HCl (Figure 5). A comparison of the WT and W− spectra in the absence of the denaturant reveals that about 75% of the signal at 278 nm in the WT PGK CD spectrum is contributed by tyrosines and only 25% by tryptophans. A small difference in the 290−300 nm region, where overlap with tyrosine bands is negligible, can be ascribed to tryptophans.

For WT PGK, which undergoes a highly cooperative, two-state unfolding transition centered at 0.77 M Gdn-HCl (Szpikowska et al., 1994), significant changes in the near-UV CD spectrum do not occur until the concentration of Gdn-HCl exceeds 0.5 M. Once the concentration of Gdn-HCl exceeds 1.0 M the spectrum is virtually featureless above 270 nm, suggesting a complete loss of tertiary structure.

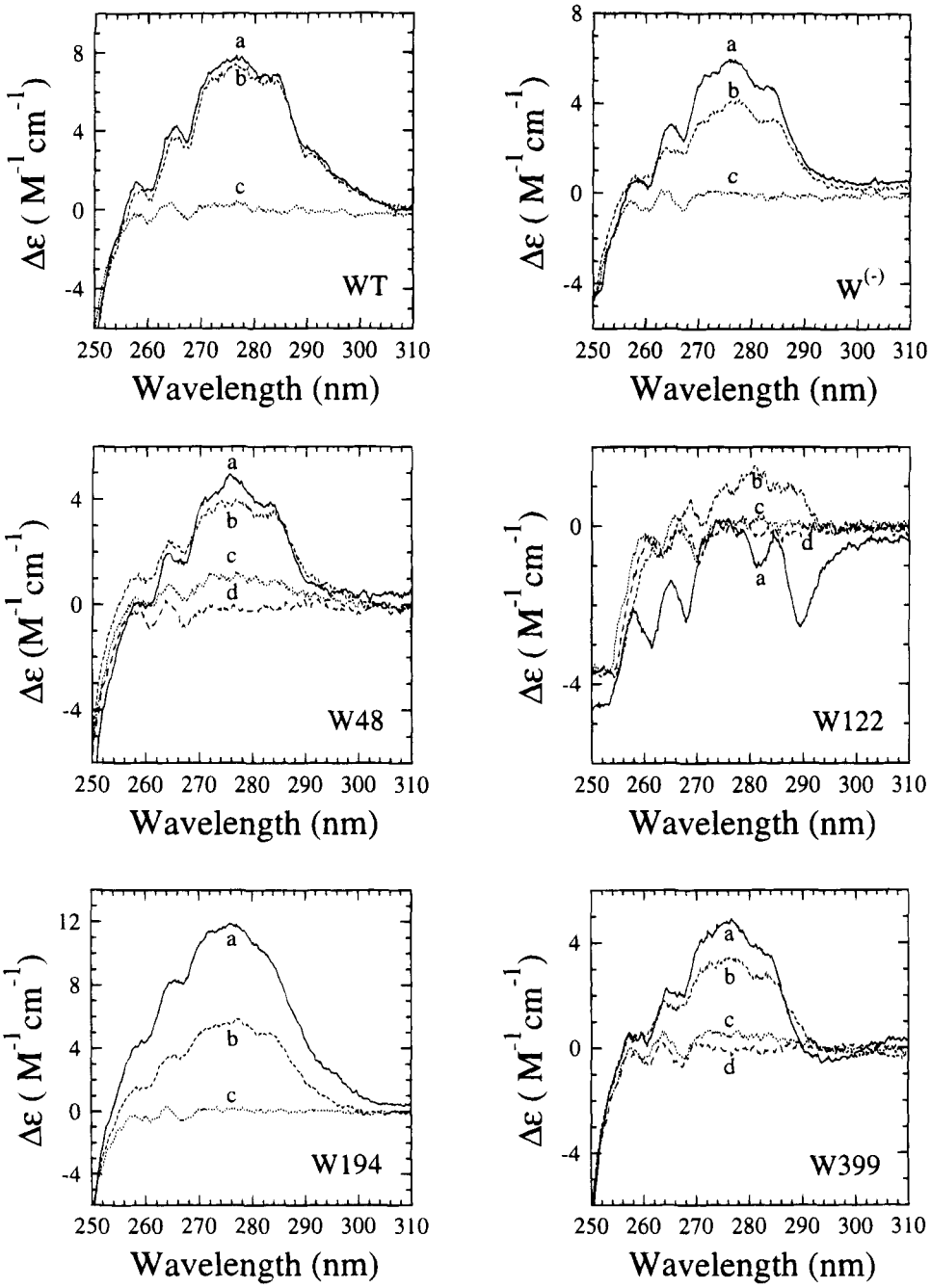

FIGURE 5: Guanidine hydrochloride induced changes in the near-UV CD spectra of WT PGK and selected mutants: (a) spectrum obtained in the absence of denaturant; (b) spectrum obtained in the presence of [Gdn-HCl] = 0.5 M; (c) [Gdn-HCl] ≥ 1.0 M; and (d) [Gdn-HCl] ≥ 1.5 M. The protein concentration for each sample was 1.0 mg/mL in 20 mM sodium phosphate, pH 7.5, at 25 °C. Spectra represent the average of 10 scans measured in a cell with a 1 cm path length.

Figure 5 shows that, for the W− and single tryptophan mutants, significant structural changes in the environment of the aromatic residues are already present at 0.5 M Gdn-HCl, as suggested by the decrease in ellipticity between 270 and 290 nm. A relatively small decrease of ellipticity in the spectrum of W− suggests perturbation of tertiary structure in the vicinity of some but not all tyrosines at 0.5 M Gdn-HCl concentration. At 1.0 M and higher Gdn-HCl concentration, a spectrum characteristic of the unfolded wild-type protein is observed. In contrast, the near-UV CD spectra of the W48, W122, and W399 mutants suggest that, even at 1.0 M Gdn-HCl, some tertiary structure remains. However, this also disappears once the concentration of Gdn-HCl exceeds 1.5 M.

DISCUSSION

We have previously described two single tryptophan containing mutants (W308 and W333) and a no-tryptophan (W−) mutant of yeast PGK, produced by replacing one or both of the C-terminal tryptophans with phenylalanines (Szpikowska et al., 1994). These mutants were constructed in order to dissect the contribution of individual tryptophans to PGK fluorescence and to monitor the equilibrium unfolding process. In the present work, genetic engineering techniques were used to introduce several new tryptophan residues (Figure 1) into a previously constructed tryptophan-less mutant (W−).

It is important to note that the unfolding behavior of the no-tryptophan, single-tryptophan, and double tryptophan

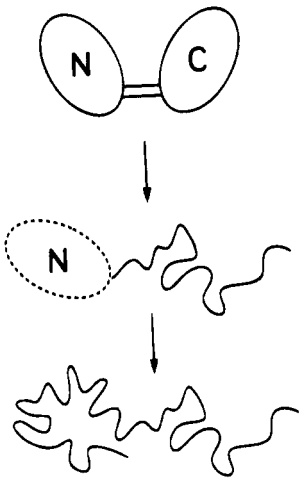

FIGURE 6: Schematic representation of the proposed unfolding pathway for yeast PGK based on the results described in this and the accompanying paper (Beecham et al., 1995). A solid line depicts folded (native) structure; a broken line, partially unfolded structure; a wavy line, unfolded structure.

PGK mutants described in this study is clearly different from that of the wild-type enzyme. In addition to a slight decrease in stability, analysis of the unfolding profiles of the mutants reveals two unfolding transitions (Figure 2), suggesting the existence of a folding intermediate under equilibrium conditions. The C_{m1} and C_{m2} values calculated for these two transitions (Table 2) are all very similar ($C_{m1} = 0.5 \pm 0.1$ M and $C_{m2} = 0.9 \pm 0.2$ M). However, the appearance of the second transition cannot be attributed to a single site-specific mutation. A second transition was also observed at ~0.9 M Gdn-HCl in the CD-monitored unfolding profile of a deletion mutant in which 15 amino acids were removed from the C-terminus of the wild-type enzyme (Mas et al., 1995). This suggests that different structural perturbations may give rise to the appearance of a second transition. The fact that the second transition is detectable only in the unfolding profiles of various mutants suggests that certain mutations might lead to an accumulation of the intermediate, perhaps by stabilizing the intermediate with respect to the folded state (Sanz & Fersht, 1993).

The results of the present study are compatible with the following equilibrium unfolding model (Figure 6): During the first transition ($C_m \sim 0.5$ M), the hinge and C-terminal domain undergo complete unfolding, while the N-terminal domain unfolds only partially. During the first transition, the N-terminal domain loses much of the tertiary structure that characterizes the native state but remains relatively compact. The second transition ($C_m \sim 0.9$ M) corresponds to a complete unfolding of the N-terminal domain.

Support for the Proposed Model: (i) Early Unfolding of the Hinge and C-Domain. When a single tryptophan is placed either in the C-domain (W308 and W333) or the hinge-spanning C-terminal peptide (W399), a single transition between 0.4 and 0.6 M Gdn-HCl is observed by tryptophan fluorescence. The fact that changes in total fluorescence and anisotropy (both of which reflect changes in the local environment of each tryptophan) coincide with the first of the CD transitions monitored at 220 nm (which reflects loss of secondary structure) suggests that the hinge and the C-domain unfold in this concentration range. Complete unfolding of the hinge alone, which consists of a single helix and the N- and C-termini, could not account for the large loss of ellipticity observed during the first transition. Therefore, other regions of the enzyme must also be unfolding during the first transition.

Hinge unfolding is also sensed by W194 located in the interdomain helix. Again, the first fluorescence-monitored transition ($C_m = 0.53$) coincides with the first CD-monitored transition ($C_m = 0.52$). In addition, near-UV CD spectra for the W399 and W194 mutants in the presence of 0.5 M Gdn-HCl are intermediate between the spectra of the folded and fully unfolded forms (Figure 5), once again suggesting that the structure of the hinge is changing rapidly in this concentration range. Further support for unfolding of the hinge and the C-domain during the first transition is provided by the time-resolved data (Figure 3), which show that, for the W308, W333, W399, and W194 mutants, the anisotropy associated with each tryptophan probe changes sharply during the first transition.

(ii) Partial Unfolding of the N-Domain. Spectral changes reported by the N-domain tryptophans suggest that partial unfolding of the N-terminal domain occurs during the first unfolding transition, thus generating a stable intermediate. As shown in Figure 2, each tryptophan in the W48 and W122 mutants experiences a large increase in total fluorescence during the first transition, followed by a large decrease during the second transition. The initial large increase suggests a change in the arrangement of local quenching groups and/or increased exposure of the probes to solvent (the latter interpretation supported by the observed 6−11 nm red-shift in wavelength of maximum fluorescence emission intensity; Table 1). It should be noted that the "hyperfluorescent intermediate" described in this study (with maximum fluorescence intensity at 0.55 M Gdn-HCl) refers to a species formed during the unfolding of the W48 and W122 mutants only and is different from the hyperfluorescent intermediate reported previously by Missiakas et al. (1990) and again recently by Garcia et al. (1995) for wild-type yeast PGK and the genetically engineered C-terminal domain (maximum fluorescence intensity at 0.9 M Gdn-HCl). Multiple experiments carried out previously in our laboratory (Szpikowska et al., 1994), and recently under conditions identical to those published by others, consistently reveal a single, highly cooperative unfolding transition for WT PGK, with no detectable intermediate.

The fact that the anisotropy properties of the N-terminal probes associated with global tumbling of the macromolecule (long rotational correlation time) fail to change during the first transition (Figure 3A) suggests that the N-domain remains compact. This is further supported by the CD data. The near-UV CD spectra recorded at 0.5 M Gdn-HCl (Figure 5) also suggest significant changes in the local environments of the W48 and W122 probes and of some, but not all, tyrosines. In addition, a substantial amount of secondary structure remains after the first transition (Figure 2), which must be attributed to the N-domain since all other experimental data suggest that the C-domain and hinge regions have already unfolded. We therefore suggest that the N-terminal domain remains partially folded during the first transition such that the core and much of its secondary structure remains intact.

The equilibrium time-resolved anisotropy titrations clearly reveal the separate nature of the first and second transitions (Figure 3). Our initial expectation was that the equilibrium time-resolved anisotropy decay (especially the slope at late times) would decrease during the unfolding of the carboxy-terminal domain. This would be the expected result if (1)

both the amino-terminal and carboxy-terminal domains were hydrodynamically coupled (i.e., rotated as a unit) in the native state and (2) unfolding of the carboxy-terminal domain uncoupled the carboxy-terminal domain from the amino-terminal domain. The time-resolved data, however, do not reveal this pattern. There is very little change in the observed rotational correlation time during this first transition region (Figure 3A). If anything, the slope of the anisotropy function at late times is actually increasing. The rotational correlation time associated with a "half-unfolded" protein may indeed be very complex, and perhaps it is not totally unexpected that the time-resolved anisotropy function does not simply decrease as the carboxy-terminal domain unfolds. The recovered long rotational correlation time in the native state is approximately 30 ns, consistent with the coupled rotational diffusion of both domains.

The fact that both genetically engineered N-domain tryptophans experience similar changes in spectral properties during the unfolding process (Figure 2), despite the large distance separating them, indicates that both residues occupy similar environments, or that the changes they experience reflect global events sensed throughout the domain. W122 is situated in a loop that packs against an adjacent loop; thus minor structural perturbations in response to low concentrations of Gdn-HCl would be sufficient to alter tertiary interactions and eliminate quenching, without significantly disrupting overall secondary structure within the domain. W48 belongs to the helix connecting β-strands A and B (Watson et al., 1982). Its tertiary interactions involve side chains contributed by the same helix and by the N-terminus; therefore, partial unfolding of the helix and/or structural changes involving the N-terminus would be sufficient to perturb tertiary interactions and eliminate quenching. Interestingly, the changes in the rotational amplitudes associated with the slow correlational time occur earlier for W122 than for W48 (Figure 4).

(iii) Complete Unfolding of the N-Domain. The final event to occur in the proposed unfolding scheme for the PGK mutants described in this paper would be complete unfolding of the N-terminal domain. This is reflected by the second transition (C_m at about 0.9 M Gdn-HCl) in the far-UV CD unfolding profiles of all the mutants studied here, as well as the second transitions seen in the fluorescence profiles of the W− mutant, and the W48, W122, and W194 single tryptophan mutants. In addition, the second transition is accompanied by a shift in the wavelength of maximum fluorescence emission to 355 nm (Table 1), the emission wavelength characteristic of a fully unfolded protein. Also, it is only at concentrations of guanidine greater than 1.0 M that one begins to observe changes in the anisotropy associated with the N-terminal probes [Figures 3 and 4 and Beechem et al. (1995)], indicating global unfolding of this domain.

(iv) Support for the Model Derived from the W48/W308 and W48/W333 Double Tryptophan Mutants. When N- and C-domain probes are placed in the same protein (W48/W333 and W48/W308), two transitions are observed both by fluorescence and by CD, similar to the transitions observed for the W48 mutant. The first fluorescence-detected transition in the double-tryptophan containing mutants ($C_m \sim 0.54$) appears to be the average of the first transitions of the corresponding single tryptophan mutants (C_m's $\sim$ 0.42 and 0.63). The major loss of ellipticity at 220 nm for each double mutant (first transition, $C_m \sim 0.53$) is also an average of the transitions of the corresponding single mutants (C_m's 0.41 and 0.65). Thus the individual probes seem to report the same conformational change when present in the single- and double-tryptophan mutants. The midpoint of the second transition for all three mutants (W48, W48/W308, and W48/W333) fails to change, remaining centered at 0.9 M Gdn-HCl. This strongly supports the notion that the first transition represents changes that occur primarily in the C-domain.

REFERENCES

Banks, R. D., Blake, C. C. F., Evans, P. R., Haser, R., Rice, D. W., Hardy, G. W., Merrett, M., & Phillips, A. W. (1979) *Nature 279*, 773−777.

Ballery, N., Minard, P., Desmadril, M., Betton, J.-M., Perahia, D., Mouawad, L., Hall, L., & Yon, J. M. (1990) *Protein Eng. 3*, 199−204.

Ballery, N., Desmadril, M., Minard, P., & Yon, J. M. (1993) *Biochemistry 32*, 708−714.

Beechem, J. M., Sherman, M. A., & Mas, M. T. (1995) *Biochemistry 34*, 13943−13948.

Betton, J.-M., Desmadril, M., Mitraki, A., & Yon, J. M. (1984) *Biochemistry 23*, 6654−6661.

Chakrabartty, A., Kortemme, T., Padmanabhan, S., & Baldwin, R. L. (1993) *Biochemistry 32*, 5560−5565.

Eftink, M. R. (1994) *Biophys. J. 66*, 482−501.

Garcia, P., Desmadril., Minard, P., & Yon, Y. M. (1995) *Biochemistry 34*, 397−404.

Gill, S. C., & von Hippel, P. H. (1989) *Anal. Biochem. 182*, 319−326.

Hitzeman, R. A., Hagie, F. E., Hayflick, J. S., Chen, C. Y., Seeburg, P. H., & Derynck, R. (1982) *Nucleic Acids Res. 10*, 7791−7808.

Kirby, E. P., & Steiner, R. F. (1970) *J. Phys. Chem. 74*, 4480−4490.

Kraulis, P. J. (1991) *J. Appl. Crystallogr. 24*, 946−950.

Manning, M. C., & Woody, R. W. (1989) *Biochemistry 28*, 8609−8613.

Mas, M. T., & Resplandor, Z. E. (1988) *Proteins: Struct., Funct., Genet. 4*, 56−62.

Mas, M. T., Chen, C. Y., Hitzeman, R. A., & Riggs, A. D. (1986) *Science 233*, 788−790.

Mas, M. T., Resplandor, Z. E., & Riggs, A. D. (1987) *Biochemistry 26*, 5369−5377.

Mas, M. T., Bailey, J. M., & Resplandor, Z. E. (1988) *Biochemistry 27*, 1168−1172.

Mas, M. T., Chen, H.-H., Aisaka, K., Lin, L.-N., & Brandts, J. F. (1995) *Biochemistry 34*, 7931−7940.

Missiakas, D., Betton, J.-M., Minard, P., & Yon, J. M. (1990) *Biochemistry 29*, 8683−8689.

Missiakas, D., Betton, J.-M., Chafotte, A., Minard, P., & Yon, J. M. (1992) *Protein Sci. 1*, 1485−1493.

Nojima, H., Ikai, A., & Noda, H. (1976) *Biochim. Biophys. Acta 427*, 20−27.

Santoro, M. M., & Bolen, D. W. (1988) *Biochemistry 27*, 8063−8068.

Sanz, J. M., & Fersht, A. R. (1993) *Biochemistry 32*, 13584−13592.

Schmid, F. X. (1989) in *Protein Structure: A Practical Approach* (Creighton, T. E., Ed.) pp 251−285, IRL Press, Oxford, U.K.

Szpikowska, B. K., Beechem, J. M., Sherman, M. A., & Mas, M. T. (1994) *Biochemistry 33*, 2217−2225.

Watson, H. C., Walker, N. P. C., Shaw, P. J., Bryant, T. N., Wendell, P. L., Fothergill, L. A., Perkins, R. E., Conroy, S. C., Dobson, M. J., Tuite, M. F., Kingsman, A. J., & Kingsman, S. M. (1982) *EMBO J. 1*, 1635−1640.

Woody, R. W. (1978) *Biopolymers 17*, 1451−1467.

BI950841W